Hedgehog-mediated patterning of the mammalian embryo requires transporter-like function of dispatched

Ma, Yong; Erkner, Alfrun; Gong, Ruoyu; Yao, Shenqin; Taipale, Jussi; Basler, Konrad; Beachy, Philip A

Hedgehog-mediated patterning of the mammalian embryo requires transporter-like function of dispatched

Abstract

The dispatched (disp) gene is required for long-range Hedgehog (Hh) signaling in Drosophila. Here, we demonstrate that one of two murine homologs, mDispA, can rescue disp function in Drosophila and is essential for all Hh patterning activities examined in the early mouse embryo. Embryonic fibroblasts lacking mDispA respond normally to exogenously provided Sonic hedgehog (Shh) signal, but are impaired in stimulation of other responding cells when expressing Shh. We have developed a biochemical assay that directly measures the activity of Disp proteins in release of soluble Hh proteins. This activity is disrupted by alteration of residues functionally conserved in Patched and in a related family of bacterial transmembrane transporters, thus suggesting similar mechanisms of action for all of these proteins.

Cell, Vol. 111, 63–75, October 4, 2002, Copyright ©2002 by Cell Press

Hedgehog-Mediated Patterning of the Mammalian Embryo Requires Transporter-like Function of Dispatched

Yong Ma,[1] Alfrun Erkner,[2] Ruoyu Gong,[1] Shenqin Yao,[1] Jussi Taipale,[1] Konrad Basler,[2] and Philip A. Beachy[1,3]
[1]Howard Hughes Medical Institute
Department of Molecular Biology and Genetics
Johns Hopkins University School of Medicine
Baltimore, Maryland 21205
[2]Institut für Molekularbiologie
Universität Zürich
Winterthurerstrasse 190
CH-8057 Zürich
Switzerland

Summary

The *dispatched* (*disp*) gene is required for long-range Hedgehog (Hh) signaling in *Drosophila*. Here, we demonstrate that one of two murine homologs, *mDispA*, can rescue *disp* function in *Drosophila* and is essential for all Hh patterning activities examined in the early mouse embryo. Embryonic fibroblasts lacking mDispA respond normally to exogenously provided Sonic hedgehog (Shh) signal, but are impaired in stimulation of other responding cells when expressing Shh. We have developed a biochemical assay that directly measures the activity of Disp proteins in release of soluble Hh proteins. This activity is disrupted by alteration of residues functionally conserved in Patched and in a related family of bacterial transmembrane transporters, thus suggesting similar mechanisms of action for all of these proteins.

Introduction

The pattern of cellular proliferation and differentiation that leads to normal development of embryonic structures often depends upon the localized production of secreted protein signals. Cells surrounding the source of a particular signal respond in a graded manner according to the effective concentration of the signal, and this response produces the pattern of cell types constituting the mature structure (Jessell, 2000; Gurdon and Bourillot, 2001). The importance in embryonic patterning of concentration-dependent cellular responses highlights in turn the importance of mechanisms that influence the effective concentration of the signaling protein. Such mechanisms include the interaction of a signaling protein with extracellular matrix, the presence and action of other interacting secreted proteins, and the sequestration and possible rerelease of the signal within the field of responding cells (Dudley and Tabin, 2000; Teleman et al., 2001).

Among secreted signaling proteins, the Hedgehog (Hh) family (Ingham and McMahon, 2001) is unique in that the mature active form of the signal (HhNp, for *N*-terminal, *p*rocessed domain) is dually lipid modified, with an ester-linked carboxy-terminal cholesteryl moiety (Porter et al., 1996b) and an amide-linked amino-terminal palmitate (Pepinsky et al., 1998). Cholesterol addition results from an autoprocessing reaction undergone by the Hedgehog protein precursor (Lee et al., 1994; Porter et al., 1996b), and palmitoylation, which is critical for signaling activity of the Hh protein, requires action of the Skinny hedgehog (Ski) acyltransferase (Chamoun et al., 2001; Lee and Treisman, 2001). Efficient addition of palmitate depends upon prior cholesterol addition, and truncated Hh proteins that are not cholesterol modified show poor activity in embryos (Lewis et al., 2001) unless expressed at high levels (Porter et al., 1996a).

Despite dual lipid modification, which might be expected to firmly anchor HhNp to the membranes of producing cells, Hh signaling extends beyond immediately adjacent cells. In the wing imaginal disc of *Drosophila*, for example, Hh production in the posterior compartment directly induces expression of the target genes *patched* (*ptc*) and *decapentaplegic* (*dpp*) in a band extending 5–10 cells beyond the boundary of Hh protein expression (Hidalgo and Ingham, 1990; Basler and Struhl, 1994; Capdevila and Guerrero, 1994). The range of direct Hh signaling is even greater in vertebrate embryos, where the mature form of the Sonic hedgehog protein (ShhNp), also dually lipidated, extends its influence many cells beyond its source to globally influence development throughout a tissue or structure. In the developing neural tube, for example, direct responses to Sonic hedgehog (Shh) are required for induction of diverse neuronal types throughout the ventral half of the neural tube (Roelink et al., 1995; Jessell, 2000; Briscoe et al., 2001), despite production of Shh protein exclusively in the notochord and floor plate (Roelink et al., 1995). The influence of this ventral midline source of Shh signal also extends through the paraxial mesoderm as far as the dorsal somite, where Shh directly induces *Myf5* expression in the myogenic precursors of the epaxial musculature (Borycki et al., 1999; Gustafsson et al., 2002). In addition, a long-range effect of direct Shh signaling is evident in the developing limb, where Shh expression at the posterior margin induces gradients of *Ptch* transcription and of Gli3 transcription and proteolytic processing across the limb bud, encompassing many cell diameters (Goodrich et al., 1996; Marigo et al., 1996b; Wang et al., 2000).

The long-range action of Shh in these tissues raises the question of how a dually lipidated protein signal can escape the membranes of cells in which it is produced to directly stimulate pathway activity in distant target cells. One possible clue to this puzzle derives from the identification of the *Drosophila* gene *dispatched* (*disp*) (Burke et al., 1999), which has a mutant phenotype similar to that of *hh*, and encodes a protein that is similar in sequence and transmembrane topology to the Ptc component of the Hh receptor (Nakano et al., 1989; Hooper and Scott, 1989; Marigo et al., 1996a; Goodrich et al., 1996; Stone et al., 1996; Fuse et al., 1999). Unlike Ptc, however, mutant mosaic studies indicate a requirement for Disp function exclusively in Hh-producing cells,

[3]Correspondence: pbeachy@jhmi.edu

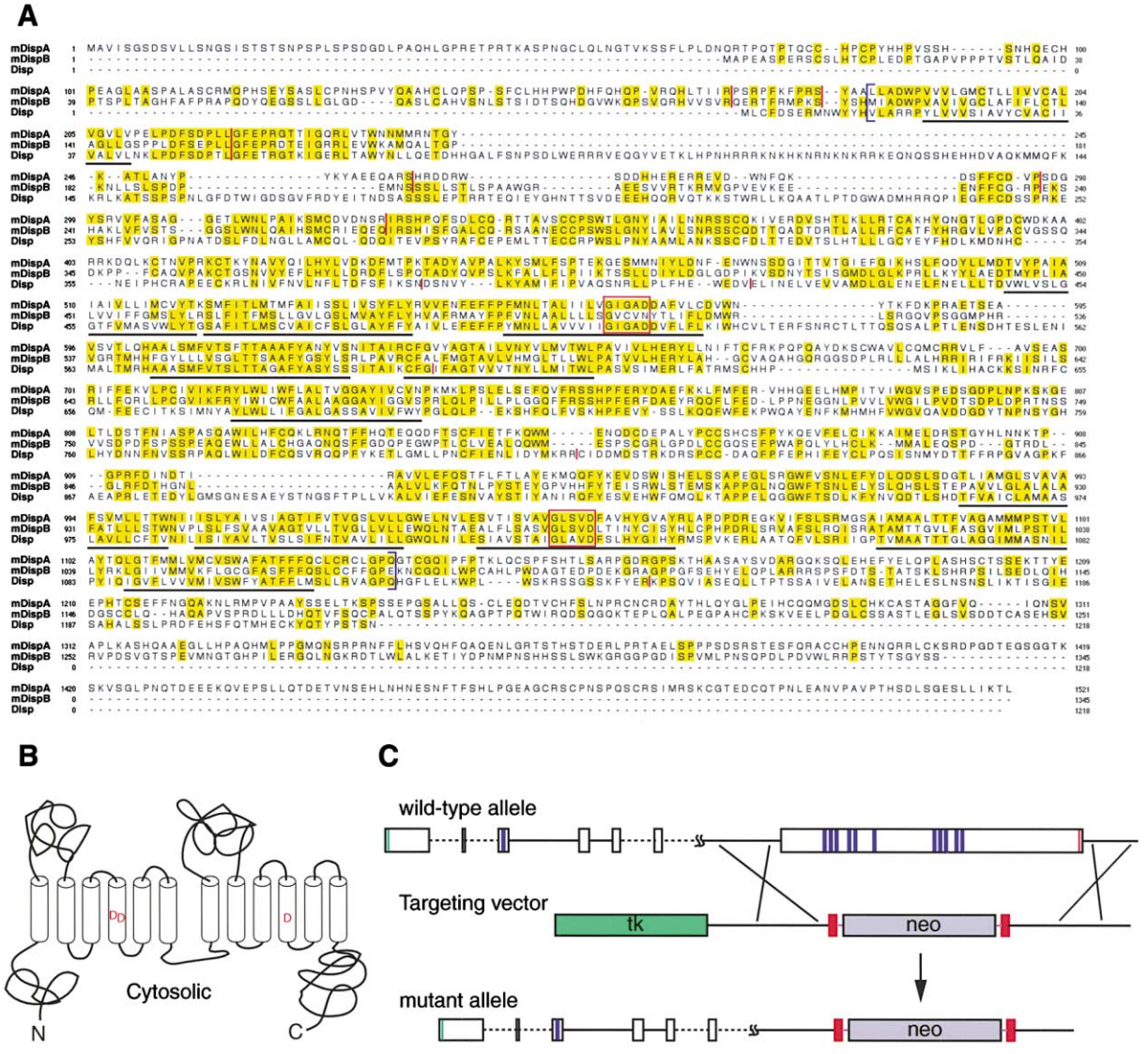

Figure 1. Characterization of Murine *dispatched* Homologs

(A) Sequence alignment between mDispA, mDispB, and *Drosophila* Disp. Identical residues are in yellow background. The twelve transmembrane spans are underlined, and the GxxxD motifs within TM4 and TM10 are in red rectangles. The intron/exon junctions are indicated by red vertical lines. Blue brackets delimit the sequences used in determining the percentages of sequence identities (see text).

(B) Proposed topology of Disp proteins. Note that the structure probably arose by tandem duplication of a six transmembrane unit. Red letters indicate the three aspartate residues within the GxxxD(D) motifs in TM4 and TM10.

(C) Generation of *mDispA* null allele. Homologous recombination of the wild-type allele with the targeting vector results in a mutant *mDispA* allele lacking a large exon coding for 11 of the 12 transmembrane domains (blue vertical lines). The seven coding exons are represented by white rectangles, and green and red vertical lines inside exons 1 and 7 indicate the start and stop codons, respectively. Thymidine kinase (tk, green rectangle) and LoxP (red box) -flanked Neo (gray box) selection cassettes are also shown. Introns of known and unknown lengths are represented by solid and dashed lines, respectively.

with loss of Disp function resulting in accumulation of the Hh signal in the producing cells and restriction of target gene expression to those cells immediately adjacent to Hh-producing cells (Burke et al., 1999). These results suggest that Disp acts by some mechanism to present or release the Hh signal for stimulation of distant target cells.

To investigate the role and mechanism of Disp protein action in mammalian Hh signaling, we characterized two murine *disp* homologs. We demonstrate that one of these, *mDispA*, is required for all detectable manifestations of Hh signaling in the patterning of the early mouse embryo. We also demonstrate in embyonic fibroblasts that a normal response to the ShhNp signal does not require mDispA function, and further show that Shh processing and modification in *mDispA* mutant cells are normal. In addition, in a direct biochemical assay of Hh export by Disp, the levels of a soluble form of Hh protein released into the medium are increased many fold upon coexpression of mammalian or *Drosophila* Disp proteins. This activity is disrupted by alteration of residues functionally conserved in Patched and in a related family

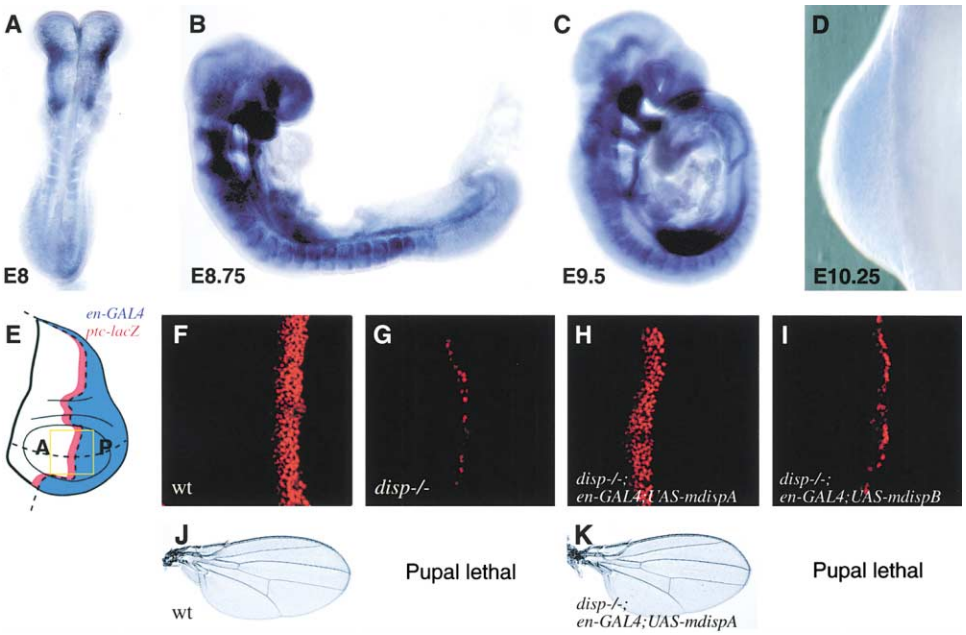

Figure 2. Early Embryonic Expression and Functional Conservation of *mDispA*, but not *mDispB*

(A–C) *mDispA* is nearly ubiquitously expressed during early embryonic development, as indicated by whole-mount in situ hybridization of wild-type embryos with antisense *mDispA* probe at E8 (A), E8.75 (B), and E9.5 (C).

(D) shows the gradient of *mDispA* message level across the hindlimb bud of E10.25 wild-type embryo (anterior is up).

(E–I) The *disp* mutation in *Drosophila* can be rescued by *mDispA*, but not by *mDispB*.

(E) Diagram of a wild-type third instar *Drosophila* wing imaginal disc. Endogenous Hh is expressed in the posterior (P) compartment, inducing a 5–10 cell wide band of anterior (A) compartment cells to express the *ptc-lacZ* reporter gene (red). Blue color indicates the pattern of *en-GAL4* driven ectopic gene expression. The yellow box demarcates the region analyzed in (F–I).

(F) shows the wide band of *ptc-lacZ* expression in wild-type wing disc. In *disp* wing discs (G), the *ptc-lacZ* expression is limited to a 1 or 2 cell wide region adjacent to the A-P boundary. This defect can be fully rescued by expression of mDispA (H) but not mDispB (I). *disp* mutants die at pupal stage (Pupal lethal), and this lethality cannot be rescued by mDispB expression. In contrast, mDispA-expressing *disp* flies develop to adulthood with normal wing pattern (compare J and K).

of bacterial transmembrane transporters, thus suggesting the possibility that all of these proteins act by similar mechanisms.

Results and Discussion

Identification of Two Murine *dispatched* Homologs

Using ESTs identified in database searches and by cDNA cloning, we characterized coding sequences for two murine homologs of *disp*, *mDispA*, and *mDispB* (Figure 1A). Based on the experimentally verified topology of the homologous protein, NPC1 (Davies and Ioannou, 2000), we propose a membrane topology for Disp that includes twelve transmembrane spans, with cytoplasmic N- and C-terminal tails (Figure 1B). The predicted amino acid sequences of Disp, mDispA, and mDispB are easily aligned, with greatest similarity noted within a continuous region that includes and extends just beyond the twelve predicted transmembrane spans (TM region; Figure 1A); little similarity occurs outside this region. Overall, the murine proteins, particularly mDispA, have larger N- and C-terminal cytoplasmic domains, whereas the *Drosophila* protein has relatively larger loops, particularly the extracellular loops between TM1 and TM2, and between TM7 and TM8.

Within the membrane-spanning region, mDispA and mDispB, respectively, display sequence identities with Disp of 36% and 31%, discounting the gaps, whereas sequence identity in this region is 42% between mDispA and mDispB. These relationships suggest that the two murine homologs duplicated after divergence of the insect and mammalian lineages. Consistent with this scenario, the coding sequences of mDispA and mDispB are identically distributed among seven exons, whereas *Drosophila* Disp coding sequences are differently distributed with only a single intron/exon junction at a point homologous to a junction in the *mDisp* genes (see Figure 1A).

Early Embryonic Expression and Functional Conservation of *mDispA*, but not *mDispB*

Given their probable duplication from a single ancestral gene, we sought to distinguish *mDispA* and *mDispB* functionally on the basis of their embryonic expression and their ability to complement *disp* mutations in *Drosophila*. By in situ hybridization, we found that the *mDispA* message is detected throughout the embryo at 7.5 days of gestation (E7.5; data not shown). This nearly ubiquitous expression of *mDispA* is maintained throughout all stages examined, albeit with some tissue-specific variations in level. Thus, for example, the level of expression at E8 is higher in the somites than in the rest of the embryo (Figure 2A), and a higher relative level of expression is observed in the branchial arches at E8.75

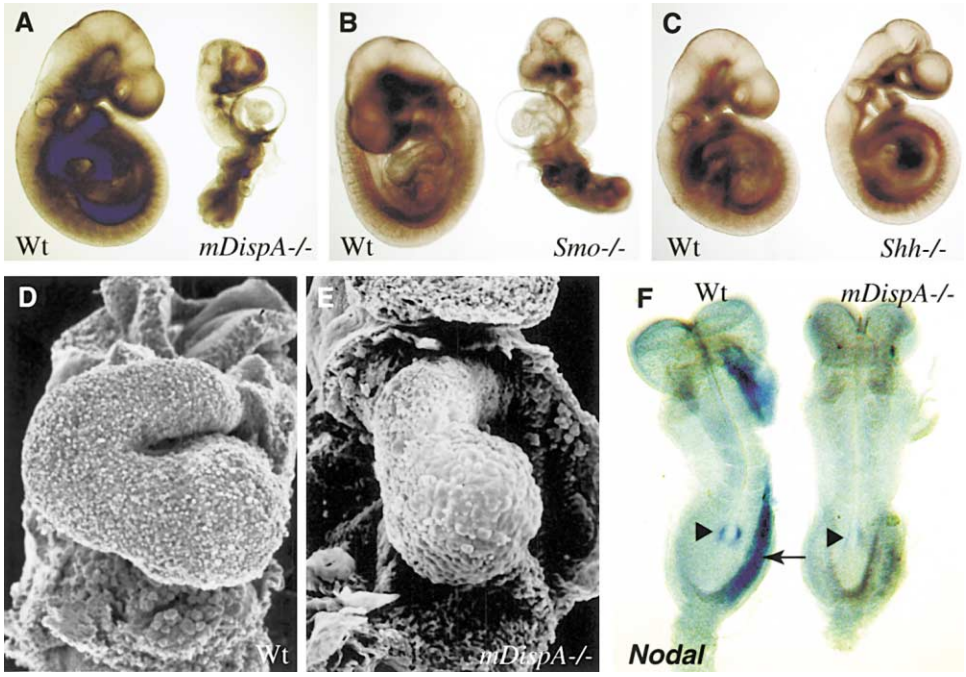

Figure 3. The Laterality Defects of *mDispA*$^{-/-}$ Embryos

(A–C) Overall morphological defects of E9.5 *mDispA*$^{-/-}$ (A), *Smo*$^{-/-}$ (B), and *Shh*$^{-/-}$ (C) embryos compared to wild-type embryos in the same litters. Note the similar phenotypes of *mDispA*$^{-/-}$ and *Smo*$^{-/-}$ embryos.

(D and E) Scanning electron micrographs of embryo hearts at E9.5, rostral is to the top. Compared to the normal rightward heart looping of a wild-type embryo (D), heart looping of a *mDispA*$^{-/-}$ embryo (E) is almost completely lost.

(F) Whole-mount in situ hybridization for *Nodal* expression at 5-6 somite stage. Whereas residual *Nodal* expression is detected in the node of *mDispA*$^{-/-}$ embryo (arrowheads), the normal *Nodal* expression in the left lateral plate mesoderm (arrow) is completely lost in the *mDispA*$^{-/-}$ embryo.

(Figure 2B) and in the limb buds at E9.5 (Figure 2C); in contrast, little expression is observed at E8.75 in the heart. A short color reaction at E10.25 reveals an apparent gradient of *mDispA* mRNA levels across the forelimb and hindlimb buds, from highest at the anterior to lowest at the posterior (Figure 2D), suggesting that *mDispA* transcription in the limb bud may be negatively regulated by signals from the posterior, such as Shh. At all the stages examined before E10, the sense strand probe for *mDispB* yielded a stronger signal than the corresponding antisense strand probe (data not shown), suggesting that *mDispB* is not expressed during the first half of gestation.

For further assessment of *mDispA* and *mDispB*, full coding sequences were tested for their ability to rescue a *disp* mutation. Although both proteins were expressed in *Drosophila* cultured cells (data not shown), their biological activities in *Drosophila* were markedly different, as expression of mDispA in Hh-producing cells restored full expression of the *ptc-lacZ* target gene in wing imaginal discs (Figure 2H, compare to Figures 2F–2G) and produced viable adults with no patterning defects (Figure 2K, compare to Figure 2J), whereas mDispB rescued neither target gene expression (Figure 2I) nor viability.

Heart Looping and Turning Defects in *mDispA* Mutant Embryos

As *mDispB* fails to rescue *Drosophila disp* and appears not to be expressed in early mouse embryogenesis, we concentrated on *mDispA* as the gene most likely to play a role in early mammalian Hh signaling. The genomic organization of the *mDispA* gene (Figure 1C) reveals that the 3′-most coding exon contains 78% of the coding sequence (1193/1521 codons), including eleven of the twelve transmembrane domains. We therefore eliminated this exon by targeted recombination (Figure 1C) in the expectation that such a deletion would cause complete loss of *mDispA* function.

We found, using this targeted allele of *mDispA*, that homozygous mutants (*mDispA*$^{-/-}$) die at or soon after E9.5 whereas heterozygotes (*mDispA*$^{+/-}$) are phenotypically wild-type. The early demise of *mDispA*$^{-/-}$ embryos suggests a phenotype more severe than that of *Shh*$^{-/-}$ embryos, which survive through most of gestation (Chiang et al., 1996). Indeed, a direct comparison at E9.5 reveals that *mDispA*$^{-/-}$ embryos (Figure 3A) are smaller than *Shh*$^{-/-}$ embryos (Figure 3C) and also carry an abnormally inflated pericardial sac and a kink in the trunk with dorsal instead of ventral curling of the tail. The *mDispA*$^{-/-}$ phenotype thus greatly resembles that of *Smoothened* mutant (*Smo*$^{-/-}$) embryos, which similarly display an inflated pericardial sac and abnormal trunk morphology (Figure 3B) due to a defect in embryonic turning. Smo is a seven transmembrane protein required for all aspects of Hh signaling (van den Heuvel and Ingham, 1996; Alcedo et al., 1996; Chen et al., 2001; Zhang et al., 2001). Embryos lacking Smo function previously were reported to show patterning defects equiv-

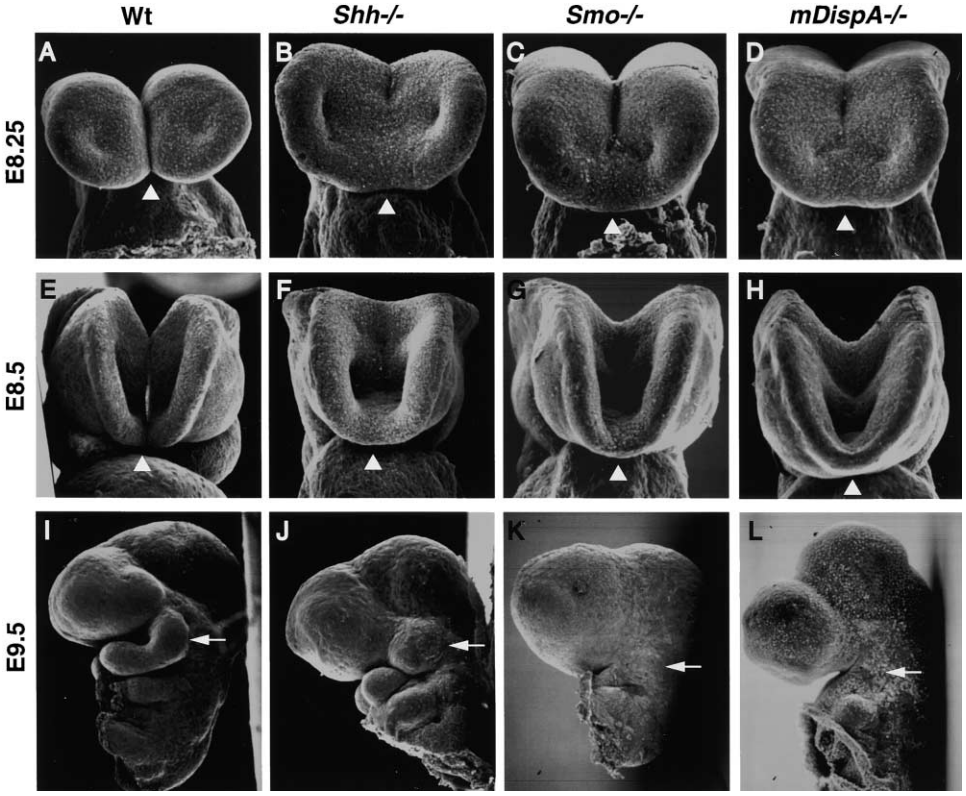

Figure 4. The Forebrain and Branchial Arch Defects of *Shh*$^{-/-}$, *Smo*$^{-/-}$, and *mDispA*$^{-/-}$ Embryos Examined by Scanning Electron Microscopy

(A–D) Frontal views of E8.25 embryo cephalic region.

(E–H) Frontal views of E8.5 embryo cephalic region.

(I–L) Lateral views of E9.5 embryo cephalic region.

(A, E, and I) Wild-type embryos.

(B, F, and J) *Shh*$^{-/-}$ embryos.

(C, G, and K) *Smo*$^{-/-}$ embryos.

(D, H, and L) *mDispA*$^{-/-}$ embryos. The midline defects of E8.25 and E8.5 forebrain are marked by arrowheads and the branchial arch defects at E9.5 are marked by arrows.

alent to those observed in embryos doubly mutant for *Shh* and *Indian hedgehog* (*Ihh*; Zhang et al., 2001). These defects include a failure to establish normal asymmetry along the left/right axis, resulting in a failure of normal embryonic turning and abnormal looping of the embryonic heart; the heart defects are probably responsible for the inflated pericardial sac and early embryonic death.

We found that left/right asymmetry in *mDispA*$^{-/-}$ embryos indeed is disrupted, as indicated by defective heart looping (compare Figures 3D and 3E). At the molecular level left/right asymmetry defects are apparent even earlier, as the normal asymmetric expression of *Nodal* in left lateral plate mesoderm (Collignon et al., 1996; Lowe et al., 1996) was disrupted in 4–8 somite stage embryos, with no expression detected in seven mutant embryos examined (Figure 3F). As noted for *Smo*$^{-/-}$ embryos (Zhang et al., 2001), expression in the node of these same embryos was variable, with three embryos displaying little expression (not shown), three displaying a somewhat higher level of expression on the left side (Figure 3F) as is characteristic of normal embryos, and one displaying a similar level of expression on right and left sides (not shown).

Early Forebrain and Branchial Arch Defects in *mDispA* Mutants

In addition to defects in left/right asymmetry, *mDispA*$^{-/-}$ embryos also display defects of the prospective head and face that are characteristic of loss of Hh signaling (Chiang et al., 1996). Thus, by the early head fold stage (E8.25; Figures 4A–4D), *Shh*$^{-/-}$, *Smo*$^{-/-}$, and *mDispA*$^{-/-}$ embryos all display common midline defects of the neural plate in the region of the prospective forebrain. These defects include midline fusion of the anterior lips of the cephalic neural plate and a poorly defined or absent midline groove and consequent incomplete separation of the bilateral evaginations that form the optic vesicles. Soon after, at ~E8.5 (Figures 4E–4H), the well-separated bilateral cup-like evaginations in the walls of the wild-type forebrain are replaced in *Shh*$^{-/-}$, *Smo*$^{-/-}$, and *mDispA*$^{-/-}$ embryos by a deep single evagination in the floor of the forebrain. It is this evagination that produces the cyclopic eye in later *Shh*$^{-/-}$ embryos, and presumably also would do so in *Smo*$^{-/-}$ and *mDispA*$^{-/-}$ embryos if their heart defects did not preclude further embryonic development.

Defects of the branchial arches are also evident in *mDispA*$^{-/-}$ embryos. In particular, the mandibular com-

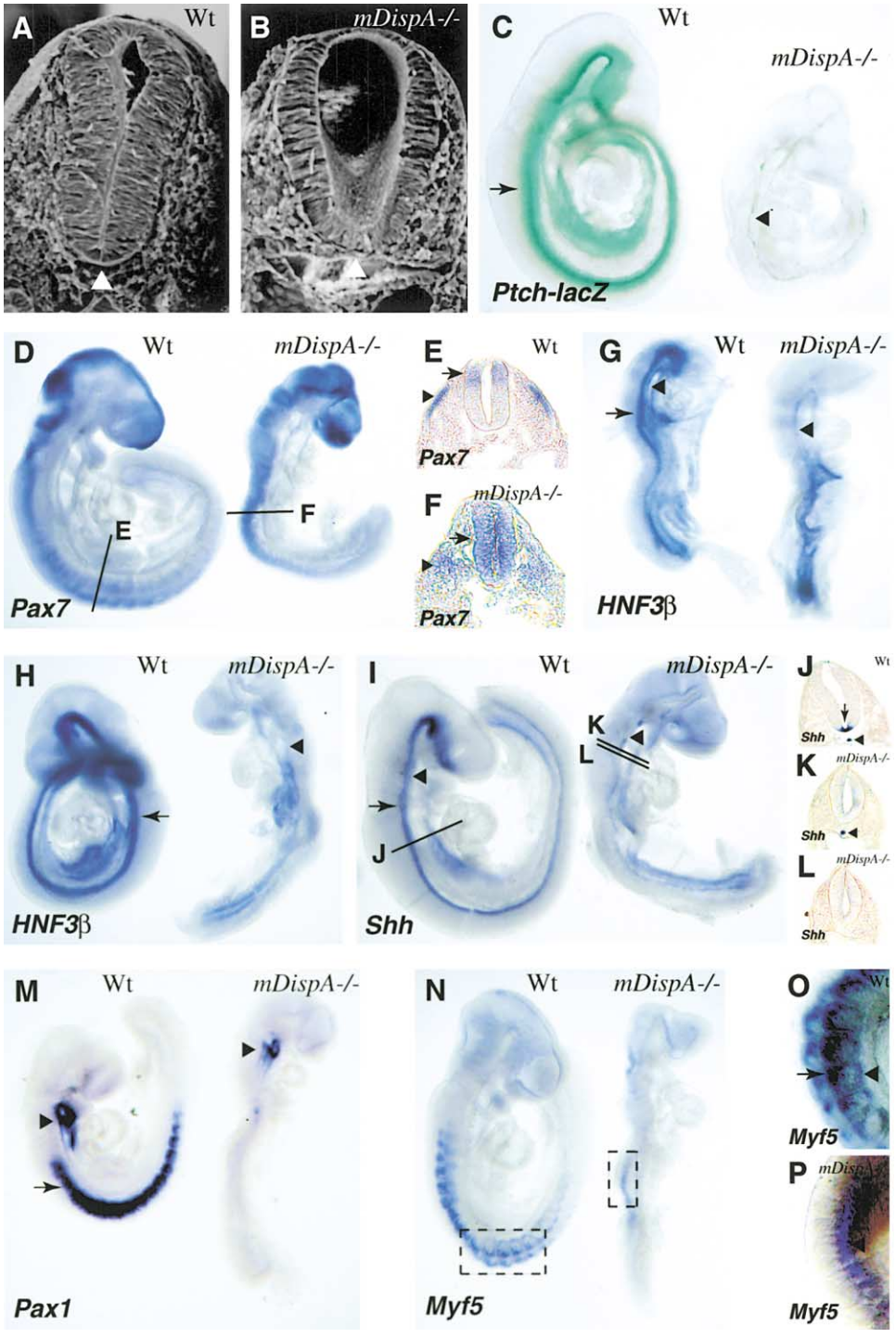

Figure 5. The Neural Tube and Somite Defects of *mDispA*$^{-/-}$ Mutants

(A and B) Scanning electron micrographs of the neural tubes of E9.5 embryos. The clearly defined morphology of the floor plate in wild-type embryo (A, arrowhead) is lost in *mDispA*$^{-/-}$ mutant (B).

(C–P) Loss of long-range Hh signaling in *mDispA*$^{-/-}$ embryos.

(C) In E9.5 *mDispA*$^{-/-}$ embryos, weak expression of a Hh pathway sensitive reporter (*Ptch-LacZ*) is retained in tissues that express Hh, such as the notochord (arrowhead) and gut. However, LacZ staining is completely lost in tissues that are farther from Hh sources, such as ventral neural tube and somites (arrow in wild-type embryo).

(D) *Pax7* expression in E9.25 embryos.

(E and F) The crosssections marked in (D) showing the ventral expansion of *Pax7* expression in both neural tube (arrow) and somites (arrowhead) in mutant embryo (F) compared to wild-type (E).

(G and H) *HNF3*β expression at E8.25 (G) and E9.25 (H). Whereas gut and weak notochord (arrowhead) expression of *HNF3*β persists at both stages, ventral neural tube expression (arrow in wild-type embryo) is not detected in *mDispA*$^{-/-}$ embryos.

ponent of the first branchial arch is severely reduced and fused in the midline (Figure 4L, compare to Figure 4I). As seen for left/right axis defects, the branchial arch defects in *mDispA*$^{-/-}$ embryos are similar to those found in *Smo*$^{-/-}$ embryos (Figure 4K), and both are more severe than the defects in *Shh*$^{-/-}$ embryos (Figure 4J), suggesting that normal development of the branchial arches may also involve Hh signaling activity other than that provided by Shh.

DISPA Is Located within HPE10, a Human Holoprosencephaly Locus

As in *Shh*$^{-/-}$ mutants, the cephalic defects in *mDispA*$^{-/-}$ embryos are reminiscent of holoprosencephaly (HPE) in humans. Holoprosencephaly encompasses a spectrum of brain and facial midline deficits that in extreme cases involve cyclopia and development of the forebrain or prosencephalon as a single undivided vesicle (Muenke and Beachy, 2001). Although heterozygous mutations in the murine *Shh* gene are silent, human *SHH* gene function is haploinsufficient and ~5% of HPE, generally at the milder end of the spectrum, can be accounted for by heterozygous *SHH* mutations (Roessler et al., 1996; Muenke and Beachy, 2001). Indeed, the *DISPA* gene is located in chromosomal region 1q42 (data not shown), which corresponds to the chromosomal interval 1q42-ter associated with HPE10 (Muenke and Beachy, 2001). It is conceivable that, despite the apparent absence of a heterozygous phenotype in the mouse, haploinsufficiency of the human *DISPA* gene could account for apparent dominant effects of chromosomal abnormalities associated with HPE10 (Muenke and Beachy, 2001).

Neural Tube Patterning Defects in *mDispA*$^{-/-}$ Mutants

Embryos lacking mDispA function also display patterning defects at more caudal levels. The ventral neural tube at the level of the presumptive spinal cord, for example, fails to take on its characteristic shape with well-differentiated floor plate cells at a sharply defined midline, and instead develops as an undifferentiated epithelial tube (compare Figures 5A and 5B). To further characterize the effects of *mDispA* loss on patterning of the neural tube and somites, we examined various genes known to depend on Hh signaling for their normal expression, and which in some cases serve as markers for the development of particular cell types.

Perhaps the most universal indicator of Hh signaling activity is the expression of *Patched* (*Ptch*) (Hidalgo and Ingham, 1990; Goodrich et al., 1996; Marigo et al., 1996b), which encodes a component of the Hh receptor and is induced by Hh signaling. We employed the murine *Ptch-lacZ* allele (Goodrich et al., 1997) to monitor pathway activity, as fusion of the *E. coli lacZ* gene in frame to the third codon of Ptch coding sequences provides a sensitive report of *Ptch* expression through histochemical staining for β-galactosidase activity. The normal expression of β-galactosidase from *Ptch-lacZ* in the ventral neural tube and somites is completely lost in the *mDispA* mutant background (Figure 5C), although continued expression in the notochord and portions of the gut suggests that some response to Hh signaling is maintained in tissues that themselves express Hh proteins (see below). We note that heterozygosity for the *Ptch-lacZ* mutant allele did not noticeably affect the abnormal morphology of *mDispA* mutant embryos. As an additional sensitive indicator of Hh protein influence we examined expression of *Pax7*, normally suppressed in the ventral neural tube by Shh that is produced in the notochord and floor plate (Fan and Tessier-Lavigne, 1994; Ericson et al., 1996). In *mDispA*$^{-/-}$ mutants, we find that the normal dorsally restricted domain of *Pax7* expression extends throughout the neural tube, including the ventral midline, suggestive of a loss of Shh signaling (Figures 5D–5F).

As markers of ventral midline structures, the *Shh* and *HNF3*-β genes normally are expressed independently of Hh signaling in the early gut and notochord and are later induced in the floor plate by Shh signaling from the notochord. In *mDispA*$^{-/-}$ embryos, normal initiation of *Shh* and *HNF3*-β expression in the notochord and gut is observed (Figures 5G–5I), but expression does not occur in the neural tube. Later expression of these markers indicates that the notochord begins to degenerate in a discontinuous fashion, much like the degeneration observed in *Shh* mutants (Chiang et al., 1996). Sections through different levels of the trunk in these embryos (Figures 5J–5L) indeed demonstrate that the notochord is absent in regions lacking *Shh* expression. Furthermore, these sections clearly demonstrate that no expression of *Shh* occurs in the neural tube, even at levels of the trunk where notochord is present and is expressing *Shh* RNA. Thus, in the *mDispA*$^{-/-}$ mutant background, expression of *Shh* in the notochord appears to be incapable of inducing normal Shh responses in the adjacent neural tube.

Somite Patterning Defects in *mDispA*$^{-/-}$ Mutants

Shh signaling normally functions to induce sclerotome, marked by expression of *Pax1* in the ventral somite (Fan and Tessier-Lavigne, 1994; Johnson et al., 1994; Fan

(I) *Shh* expression is retained in E9.5 *mDispA*$^{-/-}$ embryo in the gut and the remaining portions of the degenerating notochord (arrowhead), but not in the ventral neural tube (arrow in wild-type embryo).
(J), (K), and (L) show sections through embryos as indicated in (I). In *mDispA*$^{-/-}$ embryos, where notochord is intact (K), expression of *Shh* is comparable to that of wild-type (I), but no expression is detected in the adjacent neural tube. No *Shh* expression is detected in a section in which the notochord has degenerated (L).
(M) *Pax1* expression in E8.75 embryos. Shh induced sclerotomal expression of *Pax1* in wild-type embryo (arrow) is totally lost in a *mDispA*$^{-/-}$ mutant, whereas the Hh independent expression in the pharyngeal region (arrowhead) is not affected.
(N) *Myf5* expression in E9.25 embryos.
(O) (wild-type) and (P) (*mDispA*$^{-/-}$) are higher magnification images of the middle sections of the embryos (dashed boxes in N). Shh dependent dorsal somite expression of *Myf5* (arrow) is abolished in *mDispA*$^{-/-}$ mutant whereas Shh independent ventral somite expression (arrowhead) is not affected.

et al., 1995). Furthermore, Shh also suppresses *Pax7* expression in the ventral somite (Fan and Tessier-Lavigne, 1994), restricting it to the dorsal dermomyotome. In addition, Shh signaling contributes to dorsal somite expression of *Myf5* in the myotomal precursors of epaxial muscles (Borycki et al., 1999), and this represents one of the longest range effects that can be assigned directly to Shh signaling (Gustafsson et al., 2002). All three of these activities are disrupted in *mDispA*$^{-/-}$ embryos. Thus, sclerotomal *Pax1* expression is lost (although Hh-independent expression in the pharyngeal pouches is maintained; see Figure 5M), *Pax7* expression expands ventrally throughout the entire paraxial mesoderm (Figures 5D–5F), and the epaxial domain of *Myf5* expression in the dorsal somite is lost (Figures 5N–5P), even though a more ventral domain of Hh-independent expression of *Myf5* is maintained.

Response of *mDispA*$^{-/-}$ Cells to Hh Signaling

Although most aspects of Hh signal response appear to be disrupted in *mDispA*$^{-/-}$ embryos, some expression of the *Ptch-lacZ* reporter is retained in the notochord and in the gut at E9.25 (Figure 5C); this expression is even clearer at E8.5, before the onset of notochord degeneration (Figure 6A). The retention of *Ptch-lacZ* expression in *mDispA*$^{-/-}$ embryos would appear to represent a genuine response to Shh signaling, albeit restricted to cells that themselves express Shh, as this response is absent in *Smo*$^{-/-}$ embryos (Zhang et al., 2001). Furthermore, homozygosity for the *Ptch-lacZ* mutant allele in a *DispA* mutant background produced the abnormal morphology and widespread β-galactosidase expression characteristic of homozygous *Ptch-lacZ* mutant embryos (data not shown), indicating that mDispA functions upstream of Ptch and of signal reception, possibly in signal production. To further examine the role of mDispA function in Hh signaling, fibroblastic cell lines isolated from E8.75 *mDispA*$^{-/-}$ and *mDispA*$^{+/-}$ embryos were tested for response to exogenously added ShhNp. As monitored by Gli-luc, a luciferase reporter with eight tandem Gli binding sites (Sasaki et al., 1997; Taipale et al., 2000), heterozygous and homozygous mutant cells were both responsive to Shh signaling (Figure 6B), and this response was abrogated by the specific Hh pathway antagonist, cyclopamine (Cooper et al., 1998; Incardona et al., 1998; Taipale et al., 2000).

An intact response to Shh signaling in *mDispA*$^{-/-}$ cells indicates that the defect in embryonic patterning could be due to inappropriate cleavage and lipidation of the Shh protein or alternatively to a defect in presentation or release of the processed Shh protein. To test the ability of *mDispA*$^{-/-}$ cells to correctly process Shh, we transfected an expression construct for full-length Shh into *mDispA*$^{-/-}$ cells and compared the mobility of the protein produced to that produced by an expression construct for ShhN. The Shh expression construct encodes a full-length protein that undergoes internal cleavage and modification by cholesterol at the newly formed C terminus followed by palmitate addition at the N terminus (ShhNp). The ShhN construct contains a stop codon following the site of internal cleavage and therefore produces a protein (ShhN) containing the same amino acid residues as the processed protein but lacking cholesterol modification. We found that Shh protein expressed in *mDispA*$^{-/-}$ cells was efficiently cleaved and that its electrophoretic mobility was slightly greater than that of ShhN (Figure 6C), indicative of normal cholesterol modification (Porter et al., 1996b). This mobility was not altered by cotransfection with expression constructs for mDispA or mDispB, and these results suggest that the signaling defect in *mDispA*$^{-/-}$ embryos is not due to a defect in Shh processing.

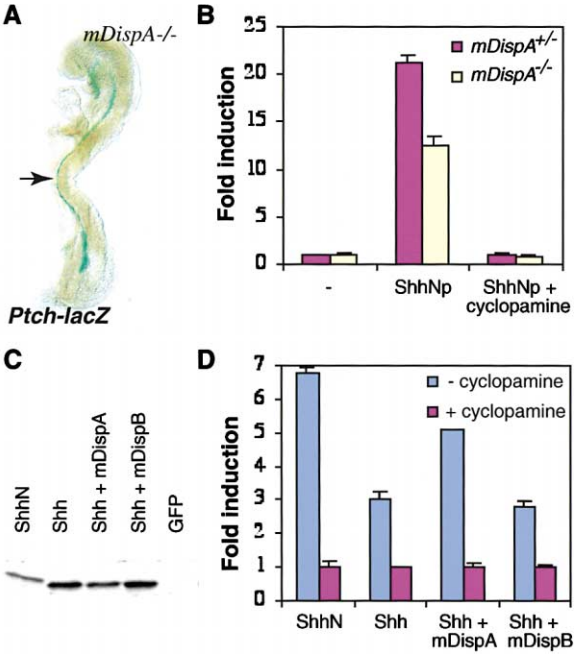

Figure 6. Cells Lacking mDispA Function Respond Normally to Shh but Fail to Efficiently Stimulate Responding Cells

(A) *mDispA*$^{-/-}$ cells are capable of responding to Hh signals, as indicated by the expression of a Hh-sensitive *Ptch-lacZ* reporter in the notochord (arrow) and gut in a E8.5 *mDispA*$^{-/-}$ embryo.

(B) *mDispA*$^{-/-}$ primary fibroblasts respond normally to exogenous Shh. *mDispA*$^{-/-}$ (yellow bars) and *mDispA*$^{+/-}$ (red bars) primary fibroblasts were transfected with Shh-sensitive Gli-luc reporter. Luciferase expression was induced in both cell lines in response to exogenously added ShhNp (10 nM), and the responses were blocked by cyclopamine (5 μM), a specific inhibitor of Shh signaling.

(C) Shh autoprocessing and cholesterol modification do not require mDispA function. *mDispA*$^{-/-}$ cells were transfected with the expression constructs indicated, and after 3 days, the electrophoretic mobilities of Shh proteins were analyzed by SDS-PAGE followed by immunoblotting. Migration of Shh N-terminal domain derived from full-length Shh construct (Shh) was not affected by coexpression of mDisp proteins and was faster than that of protein derived from truncated ShhN construct (ShhN). Because these proteins are identical in amino-acid sequence, the faster migration is indicative of cholesterol modification.

(D) Shh-expressing *mDispA*$^{-/-}$ cells fail to efficiently stimulate Hh responsive reporter cells. *mDispA*$^{-/-}$ cells were transfected with the expression constructs indicated and mixed with Shh-sensitive reporter cells (Shh-LIGHT2) in the absence or presence of cyclopamine. Transient expression of Shh alone elicited low level of response probably due to contact-dependent signaling. Coexpression of mDispA increased the response of the Shh-LIGHT2 cells to a level approaching that elicited by soluble ShhN. However, mDispB expression had no effect, consistent with the observation that mDispB cannot rescue *Drosophila disp*$^{-/-}$ mutant. Fold induction is normalized to the respective cyclopamine controls.

Defective Export of ShhNp from *mDispA*$^{-/-}$ Cells

To explore whether the *mDispA*$^{-/-}$ signaling defect is due to an inability to present or release a signaling-competent form of ShhNp, we transfected *mDispA*$^{-/-}$ mutant cells with expression constructs for full-length Shh or for ShhN and mixed these cells with stably transfected cells carrying the Gli-luc reporter (Shh-LIGHT2 cells; Taipale et al., 2000). We found that the ShhN-transfected cells induced a greater response in the Shh-LIGHT2 reporter cells (Figure 6D), consistent with previous studies demonstrating that ShhN protein is readily released from cells (Porter et al., 1996a). We tested the ability of Disp proteins to increase the amount of ShhNp available for signaling by cotransfecting the Shh expression construct into *mDispA*$^{-/-}$ cells with a construct for expression of mDispA or mDispB. We found that mDispA but not mDispB expression significantly increased the response of Shh-LIGHT2 cells (Figure 6D), suggesting that mDispA expression can increase the amount of signaling-competent Shh protein available to other cells. These experiments did not, however, distinguish between the possibilities that mDispA mediates release of ShhNp or instead mediates more efficacious presentation to responding cells on the surface of presenting cells.

To directly measure release of processed Hh proteins, we inserted coding sequences for *Renilla* luciferase in-frame into the amino-terminal signaling domains of full-length Hh and Shh coding sequences (Figure 7A). The point of insertion was a peripheral loop within the structure of ShhN (Hall et al., 1995), and the ability of Hh-Rluc and Shh-Rluc proteins to undergo processing was preserved (data not shown). We then transfected expression constructs for these modified Hh proteins together with expression constructs for Disp proteins and assayed the release of *Renilla* luciferase activity into the culture medium. Upon testing of several cell lines for Disp protein enhancement of protein export, the best results for Hh-Rluc and Shh-Rluc proteins were obtained in *Drosophila* S2 cells. In typical assays (Figure 7B), Disp proteins increased export efficiency ~3–10-fold, and enhancement of export by mouse or fly Disp was greatest for the Hh protein of the corresponding species. No enhancement of export was observed for mDispB (Figure 7B). These results indicate that Disp and mDispA, but not mDispB, can mediate the release and extracellular accumulation of Hh proteins in soluble form, and further suggest that the physiological role of Disp activity is to release Hh proteins from cells.

Functional Conservation in Disp Proteins of Residues Critical for Function of RND Transmembrane Transporters

Sequence comparison of Disp to other proteins in the database clearly shows sequence similarity not only to Ptc (Burke et al., 1999), but also to the prokaryotic RND permease superfamily. The majority of these proteins are prokaryotic efflux pumps involved in conferring resistance to drugs or heavy metals or in the secretion of endogenous molecules. These proteins appear to have arisen by tandem duplication of a six transmembrane unit (Tseng et al., 1999) to give rise to the twelve transmembrane spans of the full structure, including large extracellular loops at homologous positions in the two units, between TM1 and TM2, and between TM7 and TM8 (see Figure 1B). Biochemical studies have indicated that the RND superfamily proteins function as proton-driven antiporters (Nies, 1995; Tseng et al., 1999). Members of the RND family of proteins have a conserved GxxxD motif in the middle of TM4 (Tseng et al., 1999), and the aspartate residue within this motif is important for antiporter function and has been proposed to be the proton binding site (Goldberg et al., 1999). An expanded form of this motif, GxxxDD, is present in the middle of TM4 of Disp and mDispA, and the GxxxD motif is also present within TM10, the homologous position within the presumptive intramolecular duplication; mDispB in contrast lacks Asp within TM4 (Figure 7C).

The presence of three acidic Asp residues in the middle of the bilayer in Disp and in mDispA and the experimentally demonstrated requirement for one of these residues in the function of bacterial metal efflux pumps (Goldberg et al., 1999) suggests the possibility that Disp and the bacterial proteins might act by a similar mechanism. Consistent with this possibility, 2 of 3 of the Asp residues conserved in Disp and mDispA are absent from mDispB, which is unable to complement *Drosophila disp* mutations and unable to release Hh proteins in cultured cell assays. To further test whether these conserved Asp residues are important for the function of Disp proteins, we introduced Asn or Ala substitutions at these sites and tested expression constructs encoding these altered proteins for their ability to export Hh proteins from S2 cells. We found that neither Disp nor mDispA in either of their altered forms were able to increase export efficiency of Hh proteins when tested in the S2 cell assay (Figure 7D). To further test these altered proteins and to validate the S2 cell export assay, we tested both altered Disp proteins for their ability to rescue the *Drosophila disp* mutation in vivo. Similarly, we found that neither Disp protein carrying the Asn or the Ala substitutions was able to rescue *disp* mutant function in the wing imaginal disc (Figures 7G–7H, compare to E–F).

Conclusions

Perhaps the most striking and unexpected aspect of our results is the extreme nature of the pattern disruptions in *mDispA*$^{-/-}$ embryos. The *mDispA*$^{-/-}$ mutant phenotype is more severe than that of mutations in any single gene encoding a Hh protein (Bitgood et al., 1996; Chiang et al., 1996; St-Jacques et al., 1999). In contrast, the *Drosophila disp* mutant phenotype is less severe than the *hh* phenotype (Burke et al., 1999). This discrepancy appears in part due to disruption of signaling by multiple Hh proteins, as the *mDispA*$^{-/-}$ phenotype resembles that of *Smo*$^{-/-}$ and that of the *Shh*$^{-/-}$*; Ihh*$^{-/-}$ double mutant (Zhang et al., 2001). However, the phenotype also appears to owe its severity, at least in part, to a distinct balance in the relative importance of long-range and short-range signaling in *Drosophila* and in the mouse. In *Drosophila disp* mutants, short-range Hh signaling is intact and contributes to maintenance of target gene expression and to patterning. In *mDispA*$^{-/-}$ embryos, some signal response is retained in cells that express Shh (*Ptch-lacZ* is expressed in the notochord), but this

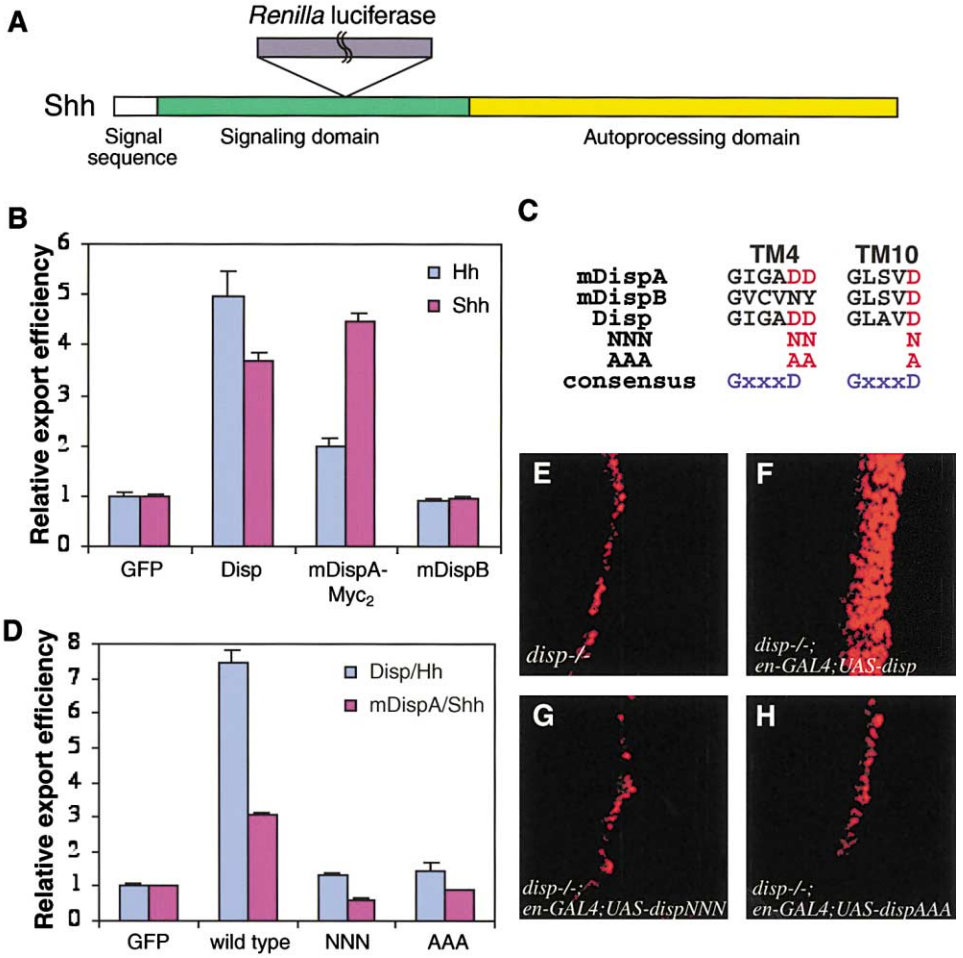

Figure 7. Transporter-Like Activity of Dispatched Exports Hh from the Producing Cell in Soluble Form

(A) The structure of Hh-*Renilla* luciferase fusion proteins used in the export assay. A secretable form of *Renilla* luciferase was generated as in Liu and Escher, 1999, and inserted into homologous sites in Shh and Hh to generate the Shh- and Hh-*Renilla* luciferase fusion proteins (Shh- and Hh-Rluc).

(B) Hh export assay in S2 cells. Both *Drosophila* Disp and mDispA increase secretion of coexpressed Hh-Rluc (blue bars) or Shh-Rluc (red bars) into the culture medium, whereas mDispB does not.

(C) Alignment of the GxxxD motif sequences of *Drosophila* Disp, mDispA, and mDispB. Residues mutated in the NNN and AAA mutant forms of both *Drosophila* Disp and mDispA are also indicated.

(D) Both the NNN and AAA mutant forms of Disp and mDispA are inactive (compare to wild-type protein and GFP control). Results from Hh and Shh export assays are shown for *Drosophila* Disp (blue bars) and mDispA (red bars), respectively.

(E–H) *Drosophila dispAAA* and *dispNNN* fail to rescue *disp* mutant phenotype. In *disp* wing disc, *ptc-lacZ* expression is limited to 1–2 cells wide region anterior to the compartment boundary (E). *en-GAL4* driven expression of wild-type Disp (F), but not DispNNN (G) or DispAAA (H), restores LacZ expression to a region comparable to that found in wild-type discs (compare F to Figure 2F).

response appears not to contribute to morphological pattern. The null function phenotype for the *mDispA* gene thus permits dissection of the relative importance of long- and short-range Hh signaling in mouse embryos and reveals a near absolute dependence on long-range signaling in patterning of the mouse embryo.

Mechanisms and processes proposed to play a specific role in long-range signaling (reviewed in Teleman et al., 2001) include the specific transport of protein signals to distant cells by movement through intervening cells (transcytosis), the sensing of signals produced at distant locations by long cytoplasmic extensions (cytonemes), and the movement of signaling proteins through tissues in membrane fragments termed argosomes (Greco et al., 2001). We can not rule out a role for Disp in helping to form these structures or mediate these processes, and these mechanisms may very well play some role in long-range action by other signaling proteins. However, the ability of Disp proteins to release soluble Hh proteins into the medium of cultured cells presents the relatively simple alternative of catalyzed signal release as a primary mechanism for initiating communication with distant cells.

The severe phenotype of the *mDispA*$^{-/-}$ mutant indicates that little Hh protein is released in the absence of Disp activity. This is perhaps not surprising, as single lipid modification of Hh protein fosters some association with cell membranes and dual lipid modification nearly quantitative association (Chamoun et al., 2001), presumably by energetically favorable insertion of the choles-

teryl and palmitoyl adducts into the lipid bilayer. Membrane release of Hh protein represents a novel activity for bacterial RND transporters, the family to which mDispA belongs. A precedent for transmembrane molecular transporter acting in release of lipid-modified proteins from membranes is that of the bacterial ATP binding cassette (ABC) transporter, the LolCDE complex of *E. coli* (Yakushi et al., 2000). Membrane release of lipoproteins also represents a novel activity for ABC transporters, as other members of this family are involved in transport of substrates across the membrane (Linton and Higgins, 1998). Like these other ABC transporters, activity of the LolCDE complex is coupled to hydrolysis of ATP, which presumably supplies the energy required for membrane release. Transmembrane transport by RND family members also requires energy in the form of an electrochemical gradient, and it will be interesting to learn whether release of Hh by Disp also depends upon such a gradient, perhaps with the use of our cultured cell system that releases soluble Hh protein. Physical characterization of protein from this system should also illuminate the question of why soluble lipidated Hh protein in the medium does not reassociate with cells and should permit comparison to other soluble forms of lipidated Hh protein (Zeng et al., 2001).

Finally, it is interesting to note that another RND family member, the Ptc protein, is a Hh pathway component that plays a central role not in Hh signal release, but in regulating response to the Hh signal by modulating the activity of Smo. Like Disp, Ptc proteins also contain a functionally conserved GxxxD motif within the predicted TM4 domain, and this motif is affected in three of the six known missense mutations that cause Basal Cell Nevus Syndrome (also Gorlin's syndrome) (Taipale et al., 2002). The Ptc protein thus also appears to function by a mechanism similar to that of Disp and RND transporters, although unlike Disp, its substrate remains unclear. These two members of the RND family with apparently similar mechanisms thus appear to have evolved to play essential yet very different roles in the Hh signaling pathway.

Experimental Procedures

Cloning and Sequence Alignments

Expressed sequence tags (ESTs) corresponding to the two murine *disp* homologs were identified by database search, and the initially identified ESTs were used to screen mouse cDNA libraries. *mDispA* cDNA was isolated as a single cDNA clone from a mouse testis cDNA library, and the full-length *mDispB* cDNA was assembled from two independent clones isolated from a mouse lung cDNA library. The accuracy of the full-length sequences was confirmed both by PCR reactions and intron/exon organization. The sequence alignment was generated using Pileup (GCG software package) and the identities between the sequences were marked by the SeqVu program.

Drosophila Stocks and Immunostaining

The *disp* mutant (*l(3)S037707*), the *UAS-disp* transgene, the *en-Gal4* driver, and the *ptc-lacZ* reporter gene are described in Burke et al., 1999. *mDispA*, *mDispB*, *myc-tagged dispNNN*, and *dispAAA* sequences were cloned into pUAST vector (Brand and Perrimon, 1993) and the corresponding UAS-transgenes were generated through P-element mediated germline transformation. $disp^{-/-}$ larvae for dissection were identified by the absence of the *Tubby* genotype present on the balancer chromosome *TM6b*. Third instar wing disc fixation and fluorescence labeling was performed as in Burke et al., 1999.

Generation and Identification of $mDispA^{-/-}$ and $Smo^{-/-}$ Mutant Alleles

The last coding exon of the *mDispA* gene was replaced by a loxP-flanked *PGK-neo* cassette through homologous recombination in the R1 ES cell line. Correctly targeted ES clones were identified by genomic Southern blot (See Supplemental Data available at http://www.cell.com/cgi/content/full/111/1/63/DC1) and chimeras were generated by blastocyst injection of C57/BL6 hosts. Germline transmission was confirmed by genotyping PCR reactions and the mutant allele was maintained in a C57/BL6;129/SvJ mixed genetic background. The $Smo^{-/-}$ mutant allele was generated by replacing part of the first coding exon of *Smo* gene including the start codon and the signal peptide by a *loxP* site through CRE-mediated site-specific recombination of a conditional *Smo* allele (to be described elsewhere). Segregation of the phenotypes with the genotypes was established using genotyping PCR reactions (See Supplemental Data available at above URL).

Probes, In Situ Hybridization, and β-Galactosidase Histochemistry

In situ hybridization and β-galactosidase histochemistry were performed essentially as described (Hogan et al., 1994; Knecht et al., 1995). *Ptch-lacZ* allele was from Dr. M. Scott. The in situ hybridization probes are as follows: two probes, AA(V3-L184) and AA(R660-Y901), were used for *mDispA* which gave essentially the same pattern; *Myf5* probe was provided by Dr. R. Emerson, and *Pax1* and *Pax7* probes were from Dr. C. Fan. *HNF3β*(3′-UTR), *Shh*(AA L373-437), and *Nodal*(3′-UTR) probes were generated by PCR reactions with mouse genomic DNA as template.

Cell Culture Based Assays

$mDispA^{-/-}$ and $mDispA^{+/-}$ embryonic fibroblasts were isolated directly from E8.75 embryos and maintained in DMEM supplemented with 10% fetal bovine serum (FBS). *Drosophila* S2 cells were maintained in Schneider's *Drosophila* Medium supplemented with 10% FBS. Fibroblasts and S2 cells were transfected using Fugene 6 (Roche) and calcium phosphate coprecipitation, respectively. For reporter assays, cell culture medium was replaced 48 hr after transfection with fresh low serum medium (DMEM with 0.5% bovine calf serum and 5 mM HEPES buffer, [pH 7.4]) containing 10 nM ShhNp and/or 5 mM cyclopamine where indicated, and after 72 hr further incubation, the cells were lysed and reporter activities measured (Dual Luciferase, Promega). For Hh/Shh-Rluc export assays, cells were collected by centrifugation 3 days after transfection and lysed directly in Passive Lysis Buffer (Promega). Conditioned medium was further cleared by centrifugation at 21,000 × g, and reporter activities in the cell lysates and conditioned medium were assayed as above. Similar results were observed using ultracentrifugation (100,000 × g for 1 hr). The relative export efficiency index was calculated using the following formula:

$$\frac{\left(\dfrac{\text{Renilla luciferase Activity in conditioned medium}}{\text{Renilla luciferase activity in cell lysate}}\right)_{+\text{Disp}}}{\left(\dfrac{\text{Renilla luciferase Activity in conditioned medium}}{\text{Renilla luciferase acitivity in cell lysate}}\right)_{-\text{Disp}}}$$

Acknowledgments

We would like to thank Drs. S.-J. Lee, C. Blobel, C.-M. Fan, and C. Emerson for R1 ES cells, libraries, and probes; Dr. M. Scott for the *Ptch-LacZ* mice; M. Cowan for blastocyst injections; and K. Young for technical assistance. We also thank Drs. S.-J. Lee, J. Nathans, G. Seydoux, and C. Machamer and members of their laboratories as well as members of the Beachy and Basler laboratories for suggestions. This work was supported by an NIH grant and by the Swiss National Science Foundation. P.A.B. is an investigator of the Howard Hughes Medical Institute.

Received: August 6, 2002
Revised: September 13, 2002
Published online: September 17, 2002

References

Alcedo, J., Ayzenzon, M., Von Ohlen, T., Noll, M., and Hooper, J.E. (1996). The *Drosophila* smoothened gene encodes a seven-pass membrane protein, a putative receptor for the hedgehog signal. Cell *86*, 221–232.

Basler, K., and Struhl, G. (1994). Compartment boundaries and the control of *Drosophila* limb pattern by hedgehog protein. Nature *368*, 208–214.

Bitgood, M.J., Shen, L., and McMahon, A.P. (1996). Sertoli cell signaling by desert hedgehog regulates the male germline. Curr. Biol. *6*, 298–304.

Borycki, A.G., Brunk, B., Tajbakhsh, S., Buckingham, M., Chiang, C., and Emerson, C.P., Jr. (1999). Sonic hedgehog controls epaxial muscle determination through Myf5 activation. Development *126*, 4053–4063.

Brand, A.H., and Perrimon, N. (1993). Targeted gene expression as a means of altering cell fates and generating dominant phenotypes. Development *118*, 401–415.

Briscoe, J., Chen, Y., Jessell, T.M., and Struhl, G. (2001). A hedgehog-insensitive form of patched provides evidence for direct long-range morphogen activity of sonic hedgehog in the neural tube. Mol. Cell *7*, 1279–1291.

Burke, R., Nellen, D., Bellotto, M., Hafen, E., Senti, K.A., Dickson, B.J., and Basler, K. (1999). Dispatched, a novel sterol-sensing domain protein dedicated to the release of cholesterol-modified hedgehog from signaling cells. Cell *99*, 803–815.

Capdevila, J., and Guerrero, I. (1994). Targeted expression of the signaling molecule decapentaplegic induces pattern duplications and growth alterations in *Drosophila* wings. EMBO J. *13*, 4459–4468.

Chamoun, Z., Mann, R.K., Nellen, D., von Kessler, D.P., Bellotto, M., Beachy, P.A., and Basler, K. (2001). Skinny hedgehog, an acyltransferase required for palmitoylation and activity of the hedgehog signal. Science *293*, 2080–2084.

Chen, W., Burgess, S., and Hopkins, N. (2001). Analysis of the zebrafish smoothened mutant reveals conserved and divergent functions of hedgehog activity. Development *128*, 2385–2396.

Chiang, C., Litingtung, Y., Lee, E., Young, K.E., Corden, J.L., Westphal, H., and Beachy, P.A. (1996). Cyclopia and defective axial patterning in mice lacking sonic hedgehog gene function. Nature *383*, 407–413.

Collignon, J., Varlet, I., and Robertson, E.J. (1996). Relationship between asymmetric nodal expression and the direction of embryonic turning. Nature *381*, 155–158.

Cooper, M.K., Porter, J.A., Young, K.E., and Beachy, P.A. (1998). Teratogen-mediated inhibition of target tissue response to Shh signaling. Science *280*, 1603–1607.

Davies, J.P., and Ioannou, Y.A. (2000). Topological analysis of Niemann-Pick C1 protein reveals that the membrane orientation of the putative sterol-sensing domain is identical to those of 3-hydroxy-3-methylglutaryl-CoA reductase and sterol regulatory element binding protein cleavage-activating protein. J. Biol. Chem. *275*, 24367–24374.

Dudley, A.T., and Tabin, C.J. (2000). Constructive antagonism in limb development. Curr. Opin. Genet. Dev. *10*, 387–392.

Ericson, J., Morton, S., Kawakami, A., Roelink, H., and Jessell, T.M. (1996). Two critical periods of sonic hedgehog signaling required for the specification of motor neuron identity. Cell *87*, 661–673.

Fan, C.M., and Tessier-Lavigne, M. (1994). Patterning of mammalian somites by surface ectoderm and notochord: evidence for sclerotome induction by a hedgehog homolog. Cell *79*, 1175–1186.

Fan, C.M., Porter, J.A., Chiang, C., Chang, D.T., Beachy, P.A., and Tessier-Lavigne, M. (1995). Long-range sclerotome induction by sonic hedgehog: direct role of the amino-terminal cleavage product and modulation by the cyclic AMP signaling pathway. Cell *81*, 457–465.

Fuse, N., Maiti, T., Wang, B., Porter, J.A., Hall, T.M., Leahy, D.J., and Beachy, P.A. (1999). Sonic hedgehog protein signals not as a hydrolytic enzyme but as an apparent ligand for patched. Proc. Natl. Acad. Sci. USA *96*, 10992–10999.

Goldberg, M., Pribyl, T., Juhnke, S., and Nies, D.H. (1999). Energetics and topology of CzcA, a cation/proton antiporter of the resistance-nodulation-cell division protein family. J. Biol. Chem. *274*, 26065–26070.

Goodrich, L.V., Johnson, R.L., Milenkovic, L., McMahon, J.A., and Scott, M.P. (1996). Conservation of the hedgehog/patched signaling pathway from flies to mice: induction of a mouse patched gene by hedgehog. Genes Dev. *10*, 301–312.

Goodrich, L.V., Milenkovic, L., Higgins, K.M., and Scott, M.P. (1997). Altered neural cell fates and medulloblastoma in mouse patched mutants. Science *277*, 1109–1113.

Greco, V., Hannus, M., and Eaton, S. (2001). Argosomes: a potential vehicle for the spread of morphogens through epithelia. Cell *106*, 633–645.

Gurdon, J.B., and Bourillot, P.Y. (2001). Morphogen gradient interpretation. Nature *413*, 797–803.

Gustafsson, M.K., Pan, H., Pinney, D.F., Liu, Y., Lewandowski, A., Epstein, D.J., and Emerson, C.P., Jr. (2002). Myf5 is a direct target of long-range Shh signaling and Gli regulation for muscle specification. Genes Dev. *16*, 114–126.

Hall, T.M., Porter, J.A., Beachy, P.A., and Leahy, D.J. (1995). A potential catalytic site revealed by the 1.7-A crystal structure of the amino-terminal signalling domain of sonic hedgehog. Nature *378*, 212–216.

Hidalgo, A., and Ingham, P. (1990). Cell patterning in the *Drosophila* segment: spatial regulation of the segment polarity gene patched. Development *110*, 291–301.

Hogan, B., Beddington, R., Costantini, F., and Lacy, E. (1994). Manipulating the Mouse Embryo: A Laboratory Manual, Second Edition, (Cold Spring Harbor, NY: Cold Spring Harbor Laboratory Press).

Hooper, J.E., and Scott, M.P. (1989). The *Drosophila* patched gene encodes a putative membrane protein required for segmental patterning. Cell *59*, 751–765.

Incardona, J.P., Gaffield, W., Kapur, R.P., and Roelink, H. (1998). The teratogenic veratrum alkaloid cyclopamine inhibits sonic hedgehog signal transduction. Development *125*, 3553–3562.

Ingham, P.W., and McMahon, A.P. (2001). Hedgehog signaling in animal development: paradigms and principles. Genes Dev. *15*, 3059–3087.

Jessell, T.M. (2000). Neuronal specification in the spinal cord: inductive signals and transcriptional codes. Nat. Rev. Genet. *1*, 20–29.

Johnson, R.L., Laufer, E., Riddle, R.D., and Tabin, C. (1994). Ectopic expression of sonic hedgehog alters dorsal-ventral patterning of somites. Cell *79*, 1165–1173.

Knecht, A.K., Good, P.J., Dawid, I.B., and Harland, R.M. (1995). Dorsal-ventral patterning and differentiation of noggin-induced neural tissue in the absence of mesoderm. Development *121*, 1927–1935.

Lee, J.D., and Treisman, J.E. (2001). Sightless has homology to transmembrane acyltransferases and is required to generate active hedgehog protein. Curr. Biol. *11*, 1147–1152.

Lee, J.J., Ekker, S.C., von Kessler, D.P., Porter, J.A., Sun, B.I., and Beachy, P.A. (1994). Autoproteolysis in hedgehog protein biogenesis. Science *266*, 1528–1537.

Lewis, P.M., Dunn, M.P., McMahon, J.A., Logan, M., Martin, J.F., St-Jacques, B., and McMahon, A.P. (2001). Cholesterol modification of sonic hedgehog is required for long-range signaling activity and effective modulation of signaling by Ptc1. Cell *105*, 599–612.

Linton, K.J., and Higgins, C.F. (1998). The *Escherichia coli* ATP-binding cassette (ABC) proteins. Mol. Microbiol. *28*, 5–13.

Liu, J., and Escher, A. (1999). Improved assay sensitivity of an engineered secreted Renilla luciferase. Gene *237*, 153–159.

Lowe, L.A., Supp, D.M., Sampath, K., Yokoyama, T., Wright, C.V., Potter, S.S., Overbeek, P., and Kuehn, M.R. (1996). Conserved left-right asymmetry of nodal expression and alterations in murine situs inversus. Nature *381*, 158–161.

Marigo, V., Davey, R.A., Zuo, Y., Cunningham, J.M., and Tabin, C.J.

(1996a). Biochemical evidence that patched is the hedgehog receptor. Nature *384*, 176–179.

Marigo, V., Scott, M.P., Johnson, R.L., Goodrich, L.V., and Tabin, C.J. (1996b). Conservation in hedgehog signaling: induction of a chicken patched homolog by sonic hedgehog in the developing limb. Development *122*, 1225–1233.

Muenke, M., and Beachy, P.A. (2001). Holoprosencephaly. In The Metabolic and Molecular Bases of Inherited Disease, C.R. Scriver, A.L. Beaudet, W.S. Sly, D. Valle, B. Childs, K.W. Kinzler, and B. Vogelstein, eds. (New York: McGraw-Hill), pp. 6203–6230.

Nakano, Y., Guerrero, I., Hidalgo, A., Taylor, A., Whittle, J.R., and Ingham, P.W. (1989). A protein with several possible membrane-spanning domains encoded by the *Drosophila* segment polarity gene patched. Nature *341*, 508–513.

Nies, D.H. (1995). The cobalt, zinc, and cadmium efflux system CzcABC from Alcaligenes eutrophus functions as a cation-proton antiporter in *Escherichia coli*. J. Bacteriol. *177*, 2707–2712.

Pepinsky, R.B., Zeng, C., Wen, D., Rayhorn, P., Baker, D.P., Williams, K.P., Bixler, S.A., Ambrose, C.M., Garber, E.A., Miatkowski, K., et al. (1998). Identification of a palmitic acid-modified form of human sonic hedgehog. J. Biol. Chem. *273*, 14037–14045.

Porter, J.A., Ekker, S.C., Park, W.J., von Kessler, D.P., Young, K.E., Chen, C.H., Ma, Y., Woods, A.S., Cotter, R.J., Koonin, E.V., and Beachy, P.A. (1996a). Hedgehog patterning activity: role of a lipophilic modification mediated by the carboxy-terminal autoprocessing domain. Cell *86*, 21–34.

Porter, J.A., Young, K.E., and Beachy, P.A. (1996b). Cholesterol modification of hedgehog signaling proteins in animal development. Science *274*, 255–259.

Roelink, H., Porter, J.A., Chiang, C., Tanabe, Y., Chang, D.T., Beachy, P.A., and Jessell, T.M. (1995). Floor plate and motor neuron induction by different concentrations of the amino-terminal cleavage product of sonic hedgehog autoproteolysis. Cell *81*, 445–455.

Roessler, E., Belloni, E., Gaudenz, K., Jay, P., Berta, P., Scherer, S.W., Tsui, L.C., and Muenke, M. (1996). Mutations in the human sonic hedgehog gene cause holoprosencephaly. Nat. Genet. *14*, 357–360.

Sasaki, H., Hui, C., Nakafuku, M., and Kondoh, H. (1997). A binding site for Gli proteins is essential for HNF-3β floor plate enhancer activity in transgenics and can respond to Shh in vitro. Development *124*, 1313–1322.

St-Jacques, B., Hammerschmidt, M., and McMahon, A.P. (1999). Indian hedgehog signaling regulates proliferation and differentiation of chondrocytes and is essential for bone formation. Genes Dev. *13*, 2072–2086.

Stone, D.M., Hynes, M., Armanini, M., Swanson, T.A., Gu, Q., Johnson, R.L., Scott, M.P., Pennica, D., Goddard, A., Phillips, H., et al. (1996). The tumour-suppressor gene patched encodes a candidate receptor for sonic hedgehog. Nature *384*, 129–134.

Taipale, J., Chen, J.K., Cooper, M.K., Wang, B., Mann, R.K., Milenkovic, L., Scott, M.P., and Beachy, P.A. (2000). Effects of oncogenic mutations in Smoothened and Patched can be reversed by cyclopamine. Nature *406*, 1005–1009.

Taipale, J., Cooper, M.K., Maiti, T., and Beachy, P.A. (2002). Patched acts catalytically to suppress the activity of Smoothened. Nature *418*, 892–896.

Teleman, A.A., Strigini, M., and Cohen, S.M. (2001). Shaping morphogen gradients. Cell *105*, 559–562.

Tseng, T.T., Gratwick, K.S., Kollman, J., Park, D., Nies, D.H., Goffeau, A., and Saier, M.H., Jr. (1999). The RND permease superfamily: an ancient, ubiquitous and diverse family that includes human disease and development proteins. J Mol. Microbiol. Biotechnol. *1*, 107–125.

van den Heuvel, M., and Ingham, P.W. (1996). Smoothened encodes a receptor-like serpentine protein required for hedgehog signalling. Nature *382*, 547–551.

Wang, B., Fallon, J.F., and Beachy, P.A. (2000). Hedgehog-regulated processing of Gli3 produces an anterior/posterior repressor gradient in the developing vertebrate limb. Cell *100*, 423–434.

Yakushi, T., Masuda, K., Narita, S., Matsuyama, S., and Tokuda, H. (2000). A new ABC transporter mediating the detachment of lipid-modified proteins from membranes. Nat. Cell Biol. *2*, 212–218.

Zeng, X., Goetz, J.A., Suber, L.M., Scott, W.J., Jr., Schreiner, C.M., and Robbins, D.J. (2001). A freely diffusible form of sonic hedgehog mediates long-range signalling. Nature *411*, 716–720.

Zhang, X.M., Ramalho-Santos, M., and McMahon, A.P. (2001). Smoothened mutants reveal redundant roles for Shh and Ihh signaling including regulation of L/R symmetry by the mouse node. Cell *106*, 781–792.

Accession Numbers

Accession numbers are AY150698 for *mDispA* and AY150699 for *mDispB*.